Journal of Alloys and Compounds 509 (2011) 2116–2126

Contents lists available at ScienceDirect

Journal of Alloys and Compounds

journal homepage: www.elsevier.com/locate/jallcom

Large-scale synthesis of bismuth sulfide nanorods by microwave irradiation

Jiliang Wu[a], Fan Qin[a], Gang Cheng[a], Hui Li[a], Jiuhong Zhang[a], Yaoping Xie[a,b], Hai-Jian Yang[b,*], Zhong Lu[a], Xianglin Yu[a], Rong Chen[a,*]

[a] Key Laboratory for Green Chemical Process of Ministry of Education and School of Chemical Engineering & Pharmacy, Wuhan Institute of Technology, Wuhan, 430073, PR China
[b] Key Laboratory of Catalysis and Materials Science of the State Ethnic Affairs Commission & Ministry of Education, College of Chemistry and Materials Science, South-Central University for Nationalities, Wuhan, 430074, PR China

ARTICLE INFO

Article history:
Received 20 August 2010
Received in revised form 22 October 2010
Accepted 27 October 2010
Available online 4 November 2010

Keywords:
Microwave irradiation
Bismuth sulfide
Nanorods
Growth mechanism

ABSTRACT

Bismuth sulfide (Bi_2S_3) has attracted considerable interest due to its potential applications in thermoelectric and electronic devices, optoelectronic devices, and biomedicine. In this study, large-scale highly crystalline Bi_2S_3 nanorods were successfully prepared from bismuth citrate and thiourea (Tu) by microwave irradiation methods. The products were characterized by powder X-ray diffraction (XRD), scanning electron microscopy (SEM), transmission electron microscopy (TEM, HRTEM) and selected area electron diffraction (SAED). The influences of reaction time, surfactants, solvents, and precursors on the formation of Bi_2S_3 nanorods were discussed. The microwave irradiation method reduced reaction time by at least 80% in the synthesis of Bi_2S_3 nanorods compared with the refluxing method. Cetyltrimethylammonium bromide (CTAB) and β-cyclodextrin (β-CD) were found to be beneficial to the formation of Bi_2S_3 nanorods. *N*,*N*-dimethylformamide, ethylene glycol, and diethylene glycol were the favorable solvents in the fabrication of these nanorods. It was found that different bismuth and sulfur precursors influenced the sizes and morphologies of the Bi_2S_3 nanorods. The proposed growth mechanism of Bi_2S_3 nanorods was also discussed.

1. Introduction

As a good semiconducting main-group metal chalcogenide with a direct energy band gap ranging from 1.2 to 1.7 eV, bismuth sulfide (Bi_2S_3) has many potential applications in the fabrication of optoelectronic and thermoelectric cooler devices, as well as in photovoltaic and thermoelectric transport, photoconductivity, electrical photoresponse, and field-emission [1–5]. Bi_2S_3 has also been proposed as a good electrode for liquid-junction solar cells [6,7]. Recently, the Weissleder and co-workers reported the use of polymer-coated Bi_2S_3 nanoparticles as injectable computed tomography (CT) imaging agent with excellent stability at high concentrations, high X-ray absorption and long circulation times in vivo [8]. It demonstrated a strong example of the biological application of Bi_2S_3. Owing to its unique properties, extensive investigation of Bi_2S_3 nanomaterials has been carried out with the development of nanotechnology. In recent years, many methods have been developed to synthesize Bi_2S_3 nanomaterials with different morphologies, such as nanotubes [9,10], nanowires [11–13], nanoribbons [14,15], nanoflowers [4,13,16], microbelts [17], snowflake-like Bi_2S_3 nanostructures [18–20] and self-supported patterns of radially aligned one-dimensional (1D) Bi_2S_3 nanostructures [21].

Among 1D Bi_2S_3 nanomaterials, Bi_2S_3 nanorods are the most extensively studied morphology. They have been fabricated through various synthetic approaches, including ionic liquid [22], solvothermal [14,23–25], hydrothermal [26–29], sonochemical [30,31], microemulsion [32] and refluxing methods [33]. However, these methods generally require rigorous experimental conditions (under a stream of N_2), long reaction time, or intricate instruments, which makes production in large scale difficult. Therefore, a simple, rapid and environment-friendly approach for the large-scale preparation of Bi_2S_3 nanorods is highly desired.

As a rapid, simple and effective heating method, microwave irradiation, with direct microwave heating of the molecular precursors, has been widely used in the synthesis of high-quality nanomaterials [34–48]. It can reduce the reaction time significantly and has the advantage of uniform heating without heating temperature gradient and lag effect [49–51]. Furthermore, microwave irradiation has a short thermal induction period with no convection processes, easy controllability, and low cost. Therefore, it is very useful in the fabrication of monodisperse nanomaterials. Currently, there are few publications relevant to the microwave synthesis of Bi_2S_3 nanomaterials. Zhu and co-worker reported the microwave-assisted synthesis of Bi_2S_3 nanorods by using an ionic liquid [22].

* Corresponding authors. Tel.: +86 13659815698; fax: +86 2787194465.
E-mail addresses: rchenhku@hotmail.com (R. Chen), yanghaijian@vip.sina.com (H.-J. Yang).

0925-8388/$ – see front matter © 2010 Elsevier B.V. All rights reserved.
doi:10.1016/j.jallcom.2010.10.160

Table 1
Experimental conditions for the preparation of Bi_2S_3 nanomaterials.

Sample	Bismuth precursor[a]	Sulfur precursor[b]	Bi/S ratio	Solvent[c]	Surfactant	Surfactant amount (g)	Reaction time (min)
R1	Bi(cit)	Tu	1:3	DMF	CTAB	0.128	30
R2	Bi(cit)	Tu	1:3	DMF	CTAB	0.128	60
R3	Bi(cit)	Tu	1:3	DMF	CTAB	0.128	90
R4	Bi(cit)	Tu	1:3	DMF	CTAB	0.128	120
S1	Bi(cit)	Tu	1:3	DMF	CTAB	0.128	5
S2	Bi(cit)	Tu	1:3	DMF	CTAB	0.128	10
S3	Bi(cit)	Tu	1:3	DMF	CTAB	0.128	15
S4	Bi(cit)	Tu	1:3	DMF	CTAB	0.128	20
S5	Bi(cit)	Tu	1:3	DMF	PVP	0.1	20
S6	Bi(cit)	Tu	1:3	DMF	β-CD	0.2	20
S7	Bi(cit)	Tu	1:3	DMF	PEG	0.1	20
S8	Bi(cit)	Tu	1:3	EG	CTAB	0.128	20
S9	Bi(cit)	Tu	1:3	DEG	CTAB	0.128	20
S10	Bi(cit)	Tu	1:3	formamide	CTAB	0.128	20
S11	Bi(cit)	Tu	1:3	ethylenediamine	CTAB	0.128	20
S12	Bi(cit)	Tu	1:3	EG	CTAB	0.128	3
S13	Bi(cit)	Tu	1:3	EG	CTAB	0.128	7
S14	Bi(cit)	Tu	1:3	EG	CTAB	0.128	13
S15	Bi(cit)	Tu	1:3	DMF	None	0	20
S16	Bi(cit)	Tu	1:3	EG	None	0	20
S17	$Bi(NO_3)_3{\cdot}5H_2O$	Tu	1:3	DMF	CTAB	0.128	20
S18	$BiCl_3$	Tu	1:3	DMF	CTAB	0.128	20
S19	Bi(cit)	Na_2S	1:3	DMF	CTAB	0.128	20
S20	Bi(cit)	$Na_2S_2O_3$	1:3	DMF	CTAB	0.128	20
S21	Bi(cit)	GSH	1:3	DMF	CTAB	0.128	20
S22	Bi(cit)	Tu	1:5	DMF	CTAB	0.128	20
S23	Bi(cit)	Tu	1:5	DMF	None	0	20

Note: **R1**–**R4** were prepared by refluxing method. All other samples were prepared by using microwave irradiation method.
[a] The molarity of bismuth precursor was 0.5 mmol.
[b] The molarity of sulfur precursor was 1.5 mmol.
[c] The volume of solvent was 35 mL.

Rod-like and urchin-like morphologies were also obtained with microwave heating [42,52–54]. However, the large-scale synthesis of high crystalline Bi_2S_3 nanorods has not been mentioned using the microwave heating method.

In our previous work, we described a refluxing method for synthesizing high crystalline and large-scale Bi_2S_3 nanorods in a two-hour timeframe [33]. Bismuth citrate, a linear polymer, assists the fabrication of Bi_2S_3 nanorods in this synthesis. In the current study, we developed the microwave heating approach to synthesize high crystalline Bi_2S_3 nanorods at large scale. By changing various experiment parameters, such as the surfactant, reaction time, solvent, reactant ratio, bismuth and sulfur precursor, different morphologies and sizes of Bi_2S_3 nanostructures were obtained. The results have helped us greatly to understand the growth mechanism of the Bi_2S_3 nanorods under microwave irradiation.

2. Experimental procedures

2.1. Materials

Bismuth citrate (Bi(cit)), polyethylene glycol (PEG, with average M_w of 10,000) and polyvinylpyrrolidone (PVP, with average M_w of 10,000) were purchased from Aldrich (USA). Cetyltrimethylammonium bromide (CTAB) was purchased from Lancaster (UK). *N*,*N*-dimethylformamide (DMF) was purchased from Bodi Chemical Reagents Co. (China). Sodium sulfite ($Na_2S_2O_3$) was purchased from Fuchen Chemical Reagents Co. (China). Formamide, β-cyclodextrin (β-CD), bismuth nitrate pentahydrate ($Bi(NO_3)_3{\cdot}5H_2O$), bismuth chloride ($BiCl_3$), ethylene glycol (EG), thiourea (Tu), sulfur (S), sodium sulfide (Na_2S), diethylene glycol (DEG) and ethylenediamine were obtained from Sinopharm Chemical Reagent Co. (China). All the reagents were analytical grade and used directly without further purification.

2.2. Synthesis of Bi_2S_3 nanomaterials by refluxing method

In a typical experiment, 0.199 g (0.5 mmol) of Bi (cit), 0.114 g (1.5 mmol) of Tu and 0.128 g (0.35 mmol) of CTAB were added to a round-bottom flask which contained 35 mL of DMF. The mixture was stirred and sonicated until all the chemicals were well-dispersed. Then the mixture was refluxed at 160 °C for 30 min in an oil bath with continuous vigorous stirring. After cooling down to room temperature, the mixture was centrifuged and a solid product was collected. The product was washed with deionized water and acetone twice, respectively. Centrifugation was subsequently conducted to collect the solid product. Finally, the product was dried in a desiccator for a few days for further characterization (R1). Samples R2–R4 were also prepared using the same method under identical condition except that the reaction time is 60, 90, and 120 min, respectively (Table 1).

2.3. Synthesis of Bi_2S_3 nanomaterials by microwave heating

In a typical experiment, 0.199 g (0.5 mmol) of Bi (cit), 0.114 g (1.5 mmol) of Tu and 0.128 g (0.35 mmol) of CTAB were added to a round-bottom flask which contained 35 mL of DMF. The mixture was stirred and sonicated until all the chemicals were well-dispersed. Then the mixed solution was heated up to 200 °C by an 800 W microwave radiation for 5 min with continuous vigorous stirring. After cooling down to room temperature, the mixture was centrifuged, washed and collected as described above (**S1**). Other samples of Bi_2S_3 nanomaterials were also prepared by microwave irradiation under identical conditions by changing the reaction time (**S2**–**S4**), surfactants (**S5**–**S7**, **S15** and **S16**), solvents (**S8**–**S14**), bismuth precursors (**S17** and **S18**), sulfur precursors (**S19**–**S21**) and the amounts of Tu (**S22** and **S23**), respectively. The detail procedure is same as described above and all the experiment parameters are listed in Table 1.

2.4. Characterization

Bi_2S_3 nanorods were characterized by powder X-ray diffraction (XRD), scanning electron microscopy (SEM), energy-dispersive X-ray (EDX), and transmission electron microscopy (TEM) techniques including high-resolution TEM imaging (HRTEM) and selected area electron diffraction pattern (SAED). XRD was carried out on Bruker AXS D8 Discover (Cu Kα = 1.5406 Å). The scanning rate is 1° min^{-1} in the 2θ range from 10° to 80°. TEM images and SAED patterns were recorded on a Philips Tecnai 20 electron microscope at an accelerating voltage of 200 kV. SEM images were taken on a LEO 1530 SEM operated at 5 kV and a Hitachi S4800 SEM at 5 eV. TEM samples were prepared by dispersing some of the solid products into ethanol and then sonicating for approximately 30 s. A few drops of the suspension were deposited on copper grids, which were then put into the desiccators for drying.

3. Results

3.1. Characterizations of Bi_2S_3 nanorods synthesized by microwave method

Fig. 1a shows powder XRD spectra of the samples prepared from Bi(cit) and Tu in DMF by different time of microwave heating in the

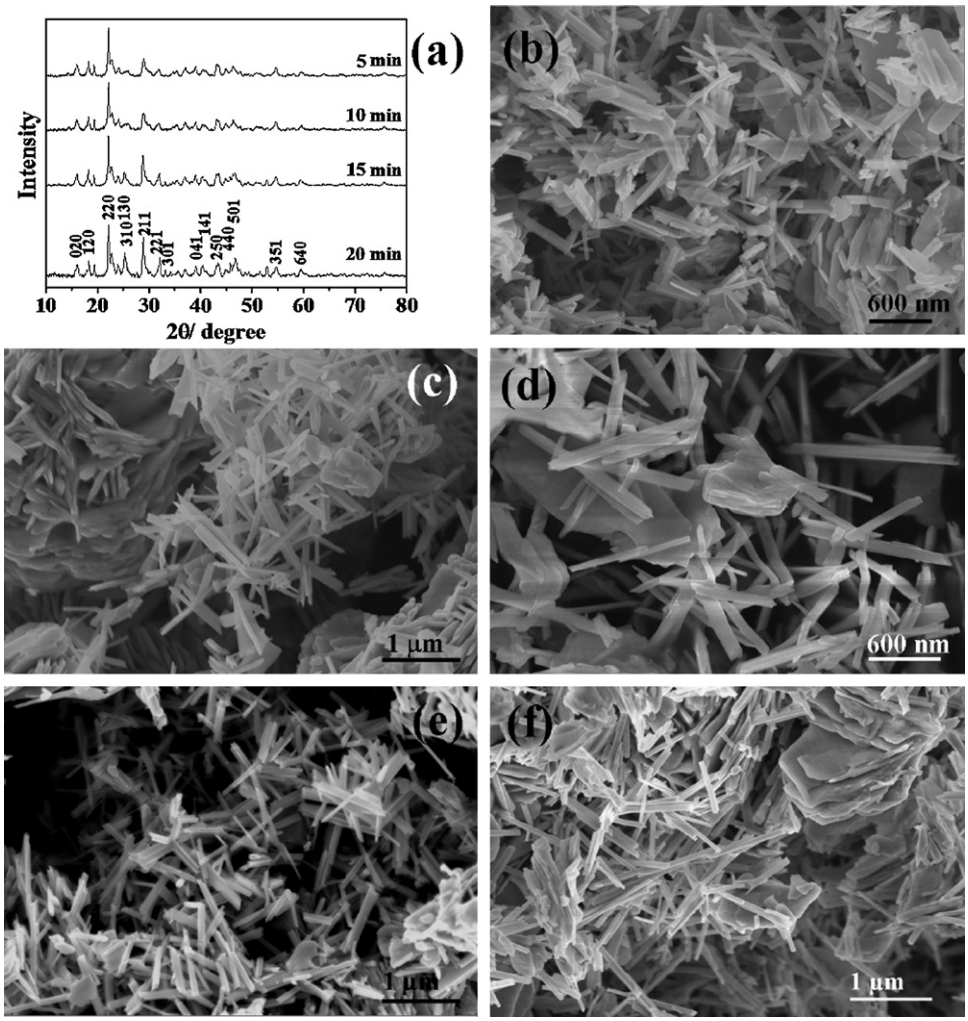

Fig. 1. Powder XRD spectra (a) and SEM images (b–f) of the products prepared from Bi(cit) and Tu by microwave heating method under different reaction time (b: 5 min; c: 10 min; d: 15 min; e: 20 min; f: 30 min).

presence of CTAB (**S1**–**S4**). All the diffraction peaks in the spectra of the four samples could be indexed to the orthorhombic phase of Bi_2S_3 (JCPDS 17-0320). No other impurities could be detected in the XRD spectra. These observations indicated that well-crystallized Bi_2S_3 can be obtained easily under this synthetic condition, even when the microwave heating time is only 5 min.

The morphology evolution of prepared Bi_2S_3 samples (**S1**–**S4**) that were obtained at different reaction time were investigated by SEM imaging, as shown in Fig. 1b–f. After only 5 min of microwave heating, rod-like Bi_2S_3 nanostructures were observed (**S1**, Fig. 1b). More and more Bi_2S_3 nanorods showed up as reaction time increased. It was observed that a large quantity (nearly 100%) of Bi_2S_3 nanorods were obtained when the reaction time was prolonged to 15 min, as shown in Fig. 1d. SEM images (Fig. 1e) displayed the uniform Bi_2S_3 nanorods with a high yield after 20 min of microwave heating. Obviously, the morphologies of the products were slightly different with the increase of reaction time. However, there was no Bi_2S_3 nanorod obtained until 90 min of refluxing had been carried out (see Supplementary Materials Fig. S1). The SEM images (Fig. S1) revealed that a large quantity of uniform Bi_2S_3 nanorods were obtained after 2 h of refluxing (**R4**), which is consistent with our reported data [33].

The structures of the Bi_2S_3 nanorods prepared by microwave heating (**S1**–**S4**) were further characterized by TEM images and SAED pattern. Similar to the SEM images, Bi_2S_3 nanorods can be detected in the sample after 5 min microwave heating. The aspect ratio, which is the average ratio of the length to the diameter of nanorods, was about 6, 7, 9 and 11, respectively (see Supplementary Materials Fig. S2). The diameter of these nanorods varied from 20 to 90 nm and the length was less than 1 μm when the reaction time was less than 20 min. The Bi_2S_3 nanorods had equal diameter (about 50 nm) after 20 min microwave heating and the length reached several micrometers. However, other morphologies of Bi_2S_3 were also observed in the whole sample (see Supplementary Materials Fig. S2). For example, Bi_2S_3 nanoparticles of less than 50 nm were obtained, which had a tendency to assemble into nanorods. Fig. 2 shows the TEM, HRTEM images and SAED pattern of the Bi_2S_3 nanorods prepared by 20 min of microwave heating (**S4**). The low-magnification TEM image (Fig. 2a) clearly revealed well-defined rod morphology. The length of the nanorods varies from 500 nm to more than 1 μm. The diameter of the Bi_2S_3 nanorods is in the range of 30–80 nm, with an average diameter of about 50 nm. The SAED pattern of Bi_2S_3 nanorods in Fig. 2b revealed several diffraction rings, which is the sum of the diffraction pattern of different individual nanorods, indicating of good crystallinity. A corresponding SAED pattern (inset of Fig. 2c) of one single nanorod was further examined and its unique pattern of diffraction spots could readily be indexed to (0 0 2) and (2 0 0) in [0 1 0] zone axis, which confirms that the nanorods examined are single crystalline and might have [0 0 1] growth direction. The preferred growth direction and the nature of the single crystallinity of the Bi_2S_3 nanorod could be verified by the HRTEM image. Fig. 2d shows a well-resolved interplanar

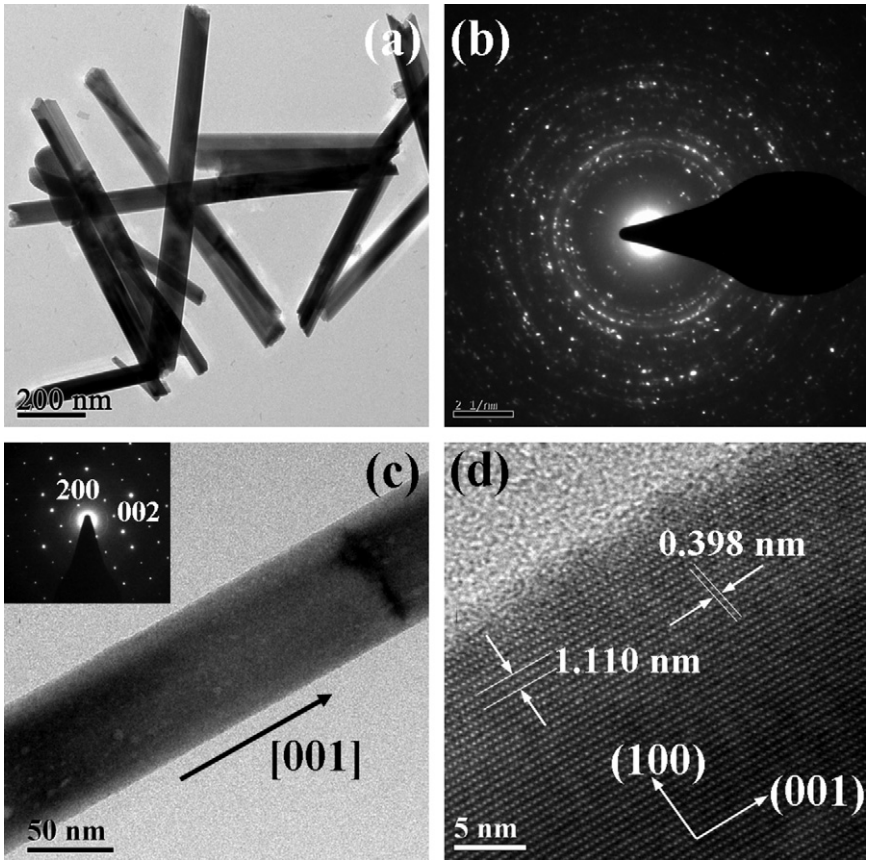

Fig. 2. Typical TEM images (a and c), SAED pattern (b) and HRTEM image (d) of Bi_2S_3 nanorods prepared by 20 min of microwave heating in DMF (S4). Inset of (c) is the SAED pattern of a selected single nanorod.

d-spacing of 1.110 and 0.398 nm, corresponding to the (1 0 0) and (0 0 1) lattice planes, respectively. The elemental compositions of the nanorods were also analyzed by EDX spectrum. It confirms that the nanorods are composed of bismuth and sulfur with an average atomic ratio of about 2:3 (see Supplementary Materials Fig. S3). The copper and carbon signals are from the carbon-coated copper grid.

An interesting result was that sheet-like Bi_2S_3 nanostructures were fabricated after 30 min of microwave heating (Fig. 1f). By increasing the reaction time, these nanorods assembled to nanorod arrays gradually, then aggregated to form the sheet-like structures. This indicates that 20 min is the optimum microwave heating time for the large scale fabrication of Bi_2S_3 nanorods.

3.2. Effect of surfactants

To investigate the effect of the surfactant on the formation of the nanorods, different surfactants were used in the synthesis of Bi_2S_3 nanorods under identical experiment conditions. Fig. 3a shows the XRD pattern of the products prepared from bismuth citrate and thiourea with 20 min microwave heating in DMF in the presence of PVP (**S5**), β-CD (**S6**), and PEG (**S7**). All the diffraction peaks can be indexed to the orthorhombic phase of Bi_2S_3 (JCPDS 17-0320), indicating the production of Bi_2S_3. Fig. 3b–d shows the SEM images of Bi_2S_3 nanostructures prepared from bismuth citrate and Tu in DMF in the presence of different surfactants, revealing differences in morphologies. When PVP was introduced into DMF (**S5**), only sheet-like Bi_2S_3 nanostructure were obtained, which can be observed in the whole sample (Fig. 3b). As shown in Fig. 3d, there are no rod-like nanomaterials observed in the presence of PEG (**S7**); only microflowers, which consisted of flakes, were obtained. However, in the presence of 5 mmol/L β-CD, large quantities of Bi_2S_3 nanorods were obtained (Fig. 3c). These nanorods were well segregated with an average diameter of about 40 nm. Nevertheless, no Bi_2S_3 nanorod was obtained when the concentration of β-CD decreased to 2.5 mmol/L or increased to 10 mmol/L (see Supplementary Materials Fig. S4).

3.3. Effect of the solvents

To understand the function of solvents in the synthesis of Bi_2S_3 nanorods, Bi_2S_3 nanomaterials were prepared by microwave heating in the presence of CTAB in EG (**S8**), DEG (**S9**), formamide (**S10**), and ethylenediamine (**S11**) under identical experiment condition, using Bi(cit) and Tu as precursors.

Fig. 4a displays the typical XRD patterns of Bi_2S_3 nanomaterials prepared in different solvents (**S8**–**S11**). The powder XRD spectra of the samples S8, S9 and S10 could be perfectly indexed to orthorhombic Bi_2S_3 (JCPDS 84-0279), (JCPDS 65-2431) and (JCPDS 06-0333), respectively. It indicated the production of crystalline pure Bi_2S_3 in the EG, DEG, and formamide. However, when ethylenediamine was used as a solvent, the powder XRD pattern was devoid of relatively sharp features, which indicated a rather isotropic nanocrystalline component of pure Bi_2S_3 [55].

The morphologies of the samples of S8–S11 were depicted by SEM images. As shown in Fig. 4b and e, a large quantity of Bi_2S_3 nanorods were obtained when EG and DEG were used as solvents (**S8** and **S9**). However, no rod-like nanomaterials were obtained in formamide and ethylenediamine. Bi_2S_3 nanoparticles and nanoplates were obtained in formamide and ethylenediamine, respectively (Fig. 4c and d). The above results showed that the solvents EG and DEG benefit the formation of Bi_2S_3 nanorods, similar to DMF.

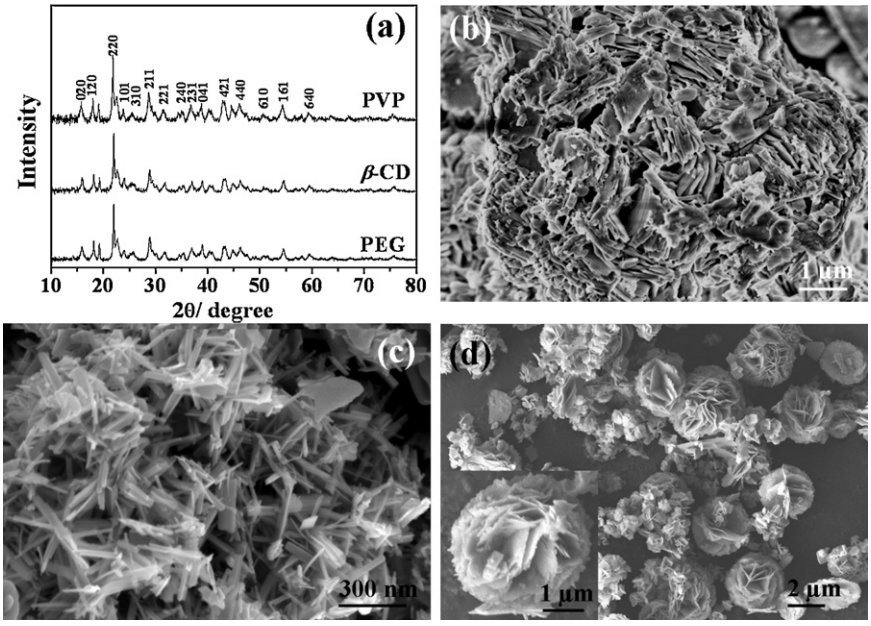

Fig. 3. Powder XRD spectra (a) and SEM images (b–d) of Bi_2S_3 nanomaterials prepared by microwave heating in DMF in the presence of PVP (b), β-CD (c) and PEG (d), respectively.

The effect of different reaction time on the formation of Bi_2S_3 nanorods in EG was also investigated. Fig. 5 showed the SEM images of as-prepared Bi_2S_3 nanorods prepared under different microwave heating time in EG (**S12**–**S14**). It revealed predominantly rod-like Bi_2S_3 nanostructures after 3 min of microwave heating. The morphologies and size of the products do not show obvious differences after 13 min of microwave heating.

Sample S8 was further characterized by TEM images and SAED pattern. Fig. 6a depicts the typical TEM image of Bi_2S_3 nanorods. The length of the nanorods varies from 200 to 800 nm, with an average

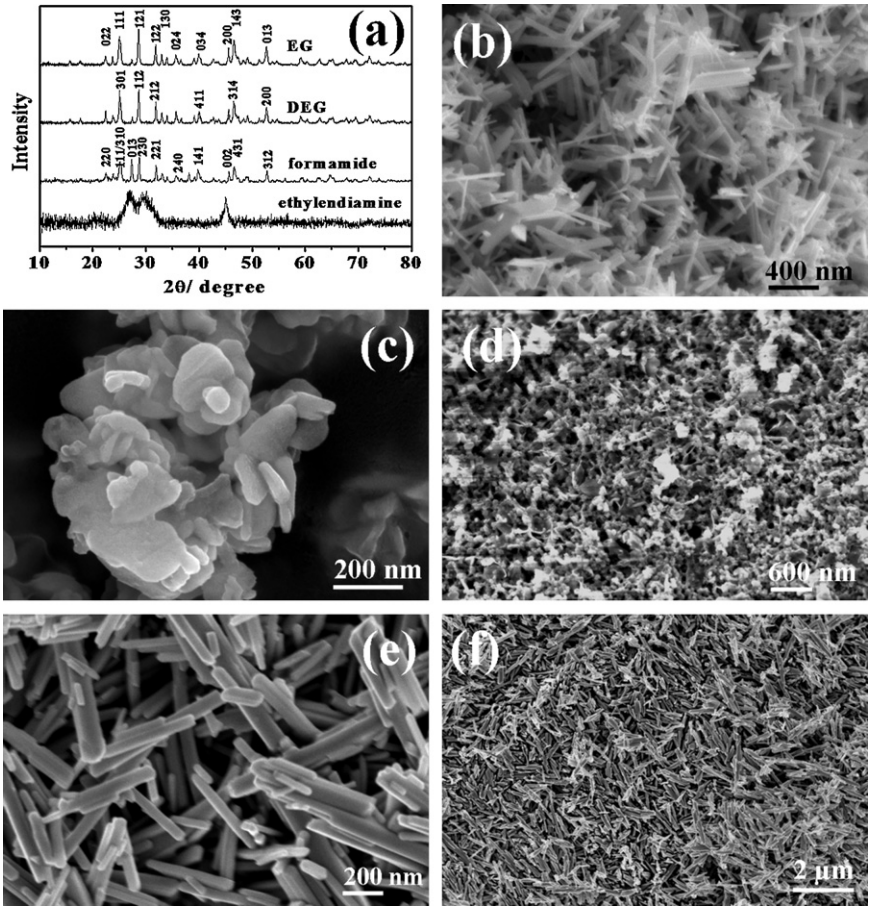

Fig. 4. Powder XRD spectra (a) and SEM images of Bi_2S_3 nanomaterials prepared by microwave heating in different solvents (b: EG; c: formamide; d: ethylenediamine; e and f: DEG).

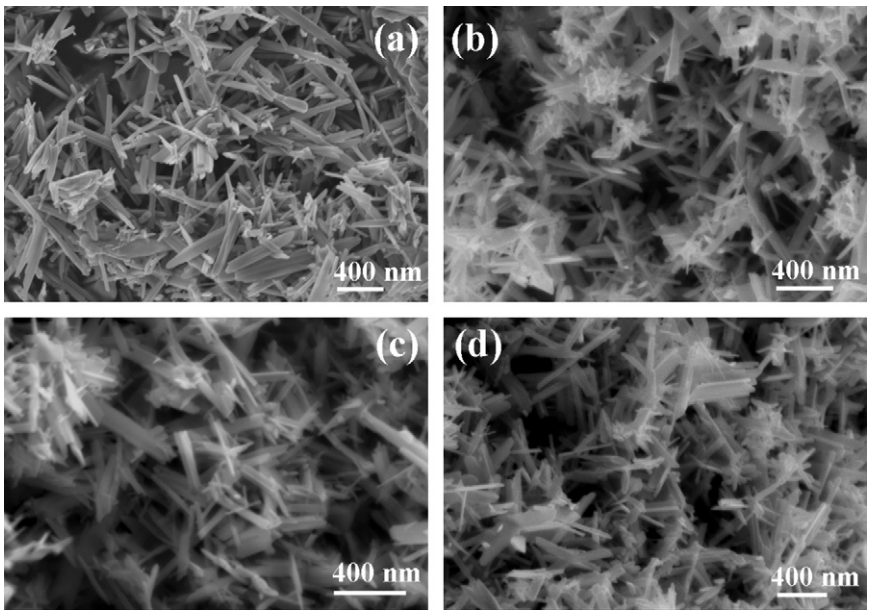

Fig. 5. SEM images of Bi_2S_3 nanorods prepared under different microwave heating time in EG (a: 3 min; b: 7 min; c: 13 min; d: 20 min).

length of about 500 nm, which is shorter than that of the nanorods fabricated in DMF. The diameters of the Bi_2S_3 nanorods are in the range of 20–70 nm, with an average diameter of about 35 nm. Fig. 6c shows the TEM images and SAED pattern of a single nanorod. The clear diffraction spots could readily be indexed to (0 0 2) and ($\bar{2}$ 2 0) in [1 1 0] zone axis, which confirms that the nanorods examined are single-crystalline and might have a [0 0 1] growth direction. The HRTEM image (Fig. 6d) reveals clear lattice fringes with *d*-spacing of 0.389 nm and 0.795 nm, which is very close to the interplanar spacing of (0 0 1) and ($\bar{1}$ 1 0), respectively.

The EDX spectra were performed for the quantitative analyses of Bi_2S_3. As shown in Fig. S5 (see Supplementary Materials), the typical EDX spectrum of Bi_2S_3 (**S11**) revealed the average atom ratio of bismuth and sulfur was approximate to 2:3, indicating of good

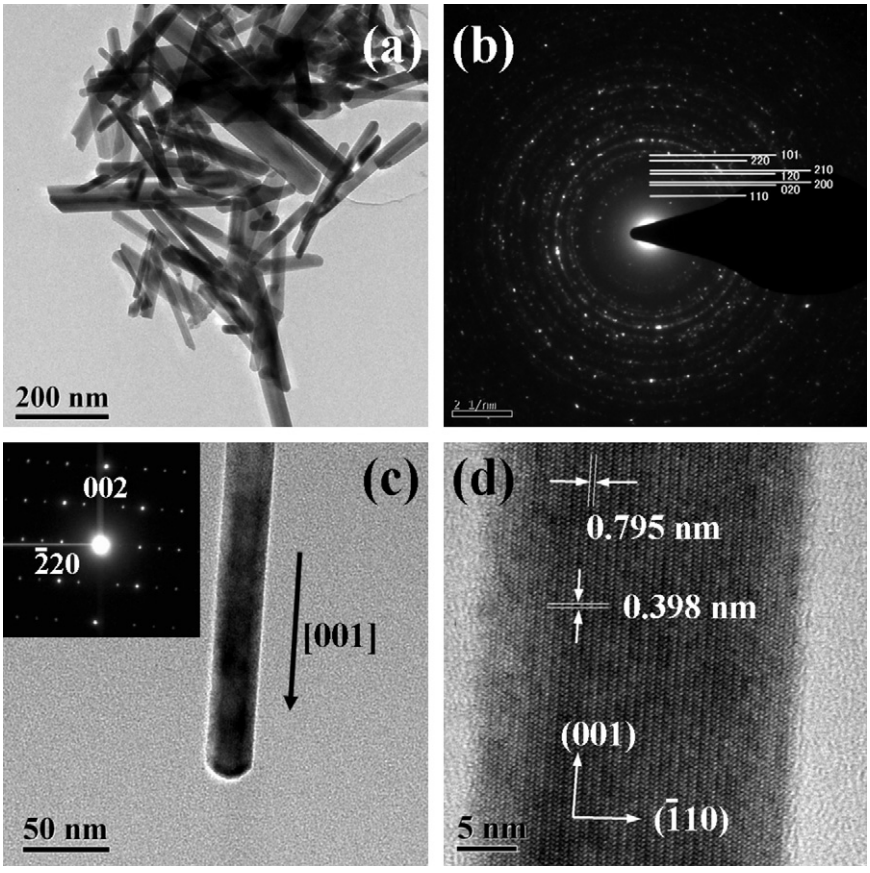

Fig. 6. Typical TEM images (a and c), SAED pattern (b) and HRTEM image (d) of Bi_2S_3 nanorods prepared by 20 min of microwave heating in EG (S8). Inset of (c) is the SAED pattern of a selected single nanorod.

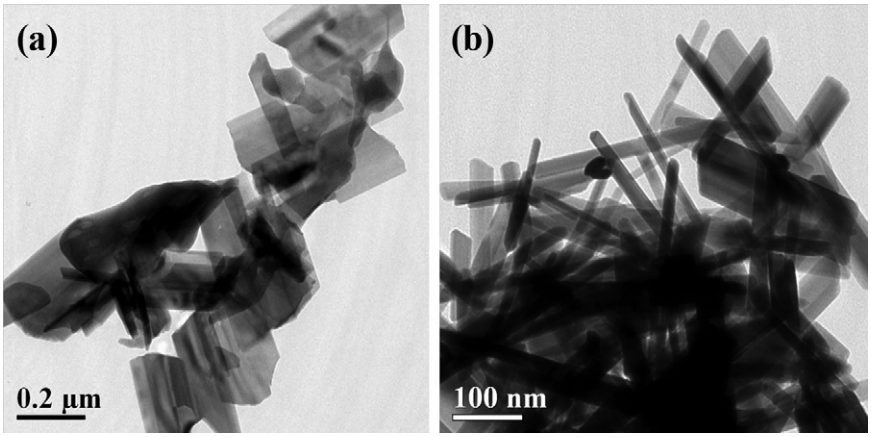

Fig. 7. TEM and SEM images of Bi_2S_3 nanorods prepared from Bi(cit) and Tu in the absence of CTAB in DMF (S15, a) and in EG (S16, b).

sample stoichiometry. The copper and carbon signals are from the carbon-coated copper grid.

The SEM and TEM images also indicated that the dispersity of Bi_2S_3 nanorods prepared in EG is little worse than that of nanorods prepared in DMF. To further investigate the effect of solvent on the dispersity of products, Bi_2S_3 nanorods were prepared under identical condition in the absence of CTAB in DMF and EG (**S15** and **S16**, respectively). As depicted in Fig. 7a, the products prepared in DMF (**S14**) have a short and wide rod-like morphology and grew to wide nanorods with a small ratio of length to diameter in the absence of CTAB in DMF, compared with the products prepared in the presence of CTAB (**S4**). However, there is no obvious difference between products prepared in the absence and presence of CTAB in EG (Fig. 7b).

To further understand the function of solvents in the formation of Bi_2S_3 nanorods, the pH value of the different solvents were measured, and qualitative analysis experiments of solubility of CTAB in different solvents were carried out. In DMF, EG, DEG, formamide, or ethylenediamine medium, the pH value is about 5, 7, 7, 9, and 12, respectively (see Supplementary Materials Fig. S6). The results of CTAB solubility showed that yellow precipitate was only observed in DMF solution, when $AgNO_3$ was added to DMF, EG, formamide and ethylenediamine solution of containing the same amount of CTAB, respectively (see Supplementary Materials Fig. S7).

3.4. Effect of precursors

In literatures, different bismuth precursors were used in the synthesis of Bi_2S_3 nanorods. For example, Chen and co-workers reported a one-step method for synthesizing high-quality single-crystalline Bi_2S_3 nanorods by thermal decomposition of $Bi[S_2P(OC_8H_{17})_2]_3$ in the presence of oleylamine [25]. Han et al. demonstrated a hydrothermal synthesis of crystalline Bi_2S_3 nanorods from Bi alkyldithiocarbonatio (xanthate) precursors [56]. Recently, BiOCl was also used as a bismuth precursor to synthesize Bi_2S_3 nanomaterials with various morphologies, including wires, rods, and flowers [57,58]. In most cases, bismuth nitrate was used as the reactant. The releasing Bi^{3+} ions can coordinate with Tu to create an environment which benefits the formation of Bi_2S_3 nanorods. In this study, $Bi(NO_3)_3$ and $BiCl_3$ was also introduced into DMF solution (**S17** and **S18**), instead of bismuth citrate. As a result, three-dimensional nanoflowers of corn-like nanorods fabricated by using $Bi(NO_3)_3$ as precursor (Fig. 8a). When $BiCl_3$ was used instead of bismuth citrate, large-scale Bi_2S_3 nanorods were also observed, as shown in Fig. 8b (**S18**). The dispersity is little worse than that of the sample prepared by bismuth citrate.

Different sulfur precursors were also introduced into the synthesis of Bi_2S_3 nanorods. $Na_2S_2O_3$, Na_2S and glutathione (γ-L-Glu-L-Cys-Gly, GSH) were used to replace Tu as the sulfur precursor (**S19**–**S21**). As shown in SEM images, petal-like morphologies of Bi_2S_3 nanomaterials were observed, using $Na_2S_2O_3$ as a sulfur source (Fig. 9a). Bulk materials were obtained when Na_2S was used as a sulfur precursor (Fig. 9b). The SEM image (Fig. 9c) demonstrated the formation of the flower-like Bi_2S_3 nanostructures which was built up of many interlaced nanoflakes in the presence of GSH. No Bi_2S_3 nanorod was obtained when $Na_2S_2O_3$, Na_2S and GSH were used as sulfur precursor, respectively.

The effect of Tu amount on the morphologies of Bi_2S_3 nanorods was also investigated. Fig. 10 shows the TEM images of Bi_2S_3 nanorods prepared by increasing the Bi(cit):Tu molar ratio to 1:5

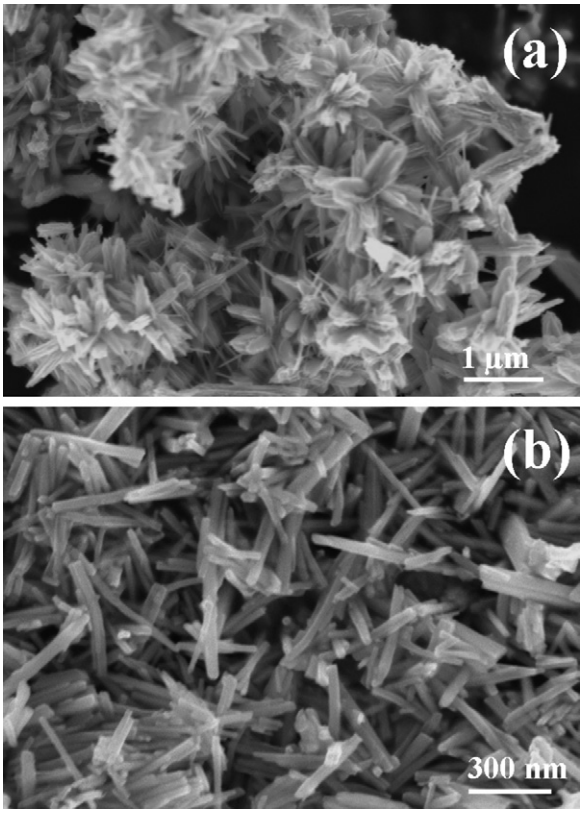

Fig. 8. SEM images of Bi_2S_3 nanomaterials prepared by using $Bi(NO_3)_3$ (a) and $BiCl_3$ (b) as bismuth precursors.

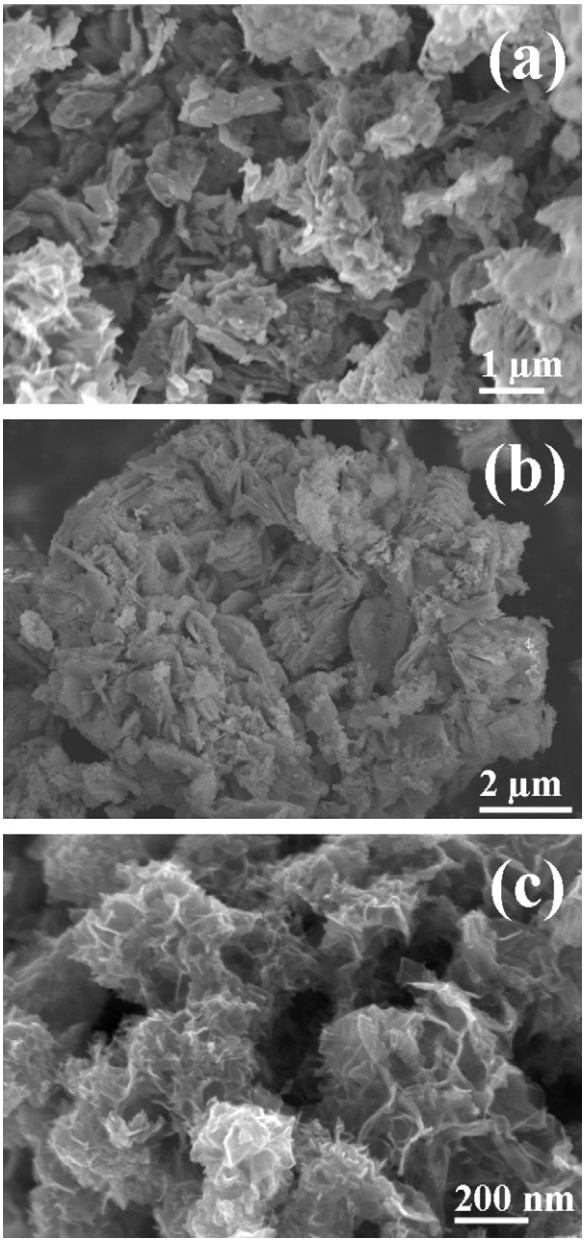

Fig. 9. SEM images (a–c) of Bi_2S_3 nanomaterials prepared from different sulfur precursors by microwave heating (a: $Na_2S_2O_3$; b: Na_2S; c: GSH).

in the presence and absence of CTAB (**S22** and **S23**, respectively). It revealed that the morphologies of as-prepared Bi_2S_3 nanorods showed obviously difference in the presence of different concentration of Tu (see Figs. 7a, and 10a, 2a and 10b). As depicted in Fig. 10, when the initial molar ratio of Bi(cit):Tu was increased to 1:5 (**S23**) in the absence of CTAB, the product still contained a large quantity of nanorods. The average aspect ratio is larger than that of those prepared by using Bi(cit):Tu molar ratio of 1:3 in the absence of CTAB (**S15**, see Fig. 7a). It was also found that the average aspect ratio increased with the increasing concentration of Tu in the presence of CTAB (**S4** and **S22**, see Figs. 2a and 10b).

4. Discussion

4.1. General discussion

Microwave irradiation, in which energy is delivered to the reactants through molecular interactions with the electromagnetic field, provides rapid and uniform heating of reagents, solvents, intermediates, and products. This rapid heating mode accelerates the reaction and nucleation in the synthesis of nanomaterials, leading to the formation of uniform, well-crystalline nanomaterials [51]. Hence, in the synthesis of Bi_2S_3 nanorods, microwave irradiation can significantly reduce reaction time by about 80%, compared to the refluxing method under identical conditions.

Formation of Bi_2S_3 nanostructures in the presence and absence of capping agent (CTAB, PVP, PEG, β-CD, etc.) has enabled us not only to understand the effect of the capping agents, but also to further determine of the growth mechanism of Bi_2S_3 nanorods. It is known that Bi_2S_3 is a highly anisotropic semiconductor with a layered structure parallel to the growth direction, with linked Bi_2S_3 units forming infinite sheets which in turn are connected via considerably weaker van der Waals interactions [59]. It consists of infinite ribbon-like (Bi_4S_6) polymers, linked together by intermolecular attraction between bismuth and sulfur atoms, which are parallel to the *c*-axis. Therefore, the preferential growth into elongated crystals is determined by the anisotropic Bi–S atom chain or layer structure of the orthorhombic Bi_2S_3 [60]. It is reported that the formation of Bi_2S_3 nanorods may have originated from the cleavage of large particles from the van der Waals planes and/or from preferential directional growth of the particles [61,62]. Growth kinetics of nanorods in the presence of capping agents is determined by several complex factors.

When CTAB was used as a surfactant, micellar solutions formed by CTAB are essential to synthesize the Bi_2S_3 nanorods. It could form double layers to control anisotropic growth, leading to the idea that the CTAB-passivated Bi_2S_3 nanorods can disperse for long

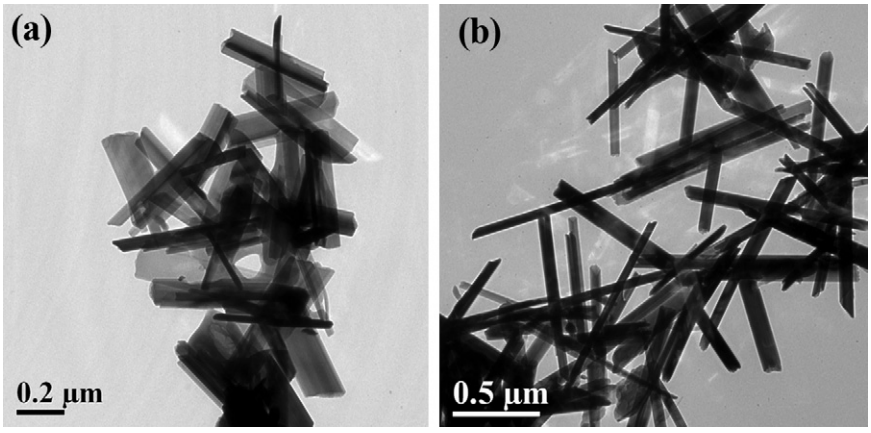

Fig. 10. TEM images of Bi_2S_3 nanorods prepared in the absence (a) and presence (b) of CTAB when the molar ratio of Bi(cit):Tu is 1:5.

periods of time without forming aggregates. This indicates that the CTAB bilayers can give good stability of the colloidal dispersion to the Bi_2S_3 nanorods. It was also proposed that CTAB capped onto the newly-formed nanorods and hence prevented the nanorods from aggregation by steric stabilization [33]. The removal of the CTAB layers tended to induce aggregation of the Bi_2S_3 nanorods.

Previous studies revealed that surfactant CTAB could act not only as a stabilizer to prevent aggregation of the crystals, but also as a shape controller to assist the formation of anisotropic metal nanostructures [63]. CTAB is a cationic surfactant consisting of a hydrocarbon chain (CTA^+) and a bromide ion (Br^-). The CTA^+ ion can adsorb onto the Bi_2S_3 surface through electrostatic effect, and acts as a capping agent to control the growth rate of the adsorbed crystal faces and to prevent those nanorods from aggregation by steric stabilization [64]. The details are shown as follows:

$$CTAB \rightarrow CTA^+ + Br^-$$

$$S^{2-} + 2CTA^+ \rightarrow (CTA^+)_2S^{2-}$$

$$3(CTA^+)_2S^{2-} + 2Bi^{3+} \rightarrow Bi_2S_3 + 6CTA^+$$

Hence, the released CTA^+ ions may have absorbed S^{2-} to form $(CTA^+)_2S^{2-}$, which prevented the production of excessive free S^{2-} ions and their quick reaction with Bi^{3+} ions, resulting in the slow production of Bi_2S_3. Once $(CTA^+)_2S^{2-}$ reacted with Bi^{3+} to form Bi_2S_3, CTA^+ also played an important role in stabilizing nanorods and reducing the surface relaxation in the formation of nanorods, resulting in well-dispersed Bi_2S_3 nanorods. CTA^+ ions can enhance the bonding strength of the adsorbed surfactant layer, which can also change the growth rate of the rods and increase surfactant capability.

PVP has a polyvinyl skeleton with polar groups, which induced an anisotropic growth of the nuclei [65]. There could also be potential crystal face inhibitors in the system, which benefits the formation of oriented nucleation, leading to the construction of anisotropic growth of the nanostructures. PVP can be adsorbed onto Bi_2S_3 nanoplates by coordinating with both nitrogen and oxygen atoms in the polar pyrrolidone groups [66]. However, the electrostatic interactions of PVP with the Bi_2S_3 surface are complicated in the formation of Bi_2S_3 nanorods. PVP can selectively cap the side facet of Bi_2S_3 nanocrystal, and thus result in different orientation attachment, which deviates from Ostwald ripening. The PVP absorption on Bi_2S_3 plane surface, which is not the growth-direction plane, suggested that there is a repulsive effect on the growth along the growth direction. A typical example is the shape control of gold and silver nanoparticles using the surfactant PVP as a capping agent, which can selectively interact with gold planes (e.g., 1 1 1, 1 0 0 and 1 1 0), and thus results in different metal nanostructures including nanorods, nanowires, nanoplates, and nanocubes [67–69].

PEG is a non-ionic polymer containing hydrophilic –O– and hydrophobic $–CH_2–CH_2–$ groups. PEG macromolecules bond with the solid surface mainly via the –OH group of nanomaterials, which may interact with PEG through hydrogen bonding. It was assumed that PEG would act as a nucleus for aggregation. Once Bi_2S_3 seeds were formed, PEG capped on the surface of Bi_2S_3 nuclei, which induced the aggregation of Bi_2S_3 nanocrystals. This may be because, in contrast to densely packed CTAB layers, PEG is amphiphilic molecules that form spontaneous molecular assemblies which in turn could act as barriers and affect the reshaping of Bi_2S_3 nanostructures [70].

The exact role of β-CD in the formation of Bi_2S_3 nanorods is still unclear, but intriguing. The morphology is strongly dependent on the concentration of β-CD in the formation of Bi_2S_3 nanomaterials. It was proposed that the viscosity of the reaction system increased with the increase of β-CD concentration, leading to the aggregation of Bi_2S_3 nanorods. However, very low concentrations can also be adverse to the dispersity of the product. This finding is in good agreement with the reported literature [71].

On the basis of the observations, it was found that different solvents have a strong influence on the Bi_2S_3 morphologies, which might be due to the decomposition of Tu in the solvents. The decomposition reaction could be represented by the following equations [72,73]:

$$(H_2N)_2C{=}S \xrightarrow{\Delta} S^{2-} + N{\equiv}CNH_2 + 2H^+$$

This illustrates that releasing of H^+ ions accompanies the generation of S^{2-} ions in the decomposition of Tu. The pH value of the reaction medium affects the balance of this reaction. The different pH values of DMF, EG, DEG, formamide, and ethylenediamine solution resulted in the different decomposition of Tu. High pH value can accelerate the decomposition of Tu, leading to the quick production of a large amount of S^{2-} ions. This accelerates the aggregation of Bi_2S_3 nuclei, which results in the formation of bulk materials.

On the other hand, it has been mentioned above that CTA^+ ions can control the formation speed and the dispersity during the growth of Bi_2S_3 nanorods. However, it was shown that there are obvious differences in morphology and dispersity among different solvents. We proposed here that the different solubility of CTAB in different solvent had a strong influence on the morphology and dispersity. Qualitative analysis experiments showed different solubility of CTAB in different solvents, indicating that only free Br^- ions from CTAB was presented in DMF solution. There were no free Br^- ions in EG, ethylenediamine, or formamide solution of CTAB, indicating of poor solubility of CTAB in these solvents. In DMF, the release of CTA^+ ions led to formation of well-separated Bi_2S_3 nanorods. That is why there was no rod-like Bi_2S_3 obtained in ethylenediamine or formamide.

Interestingly, Bi_2S_3 nanorods were obtained in EG, even with the poor CTAB solubility or without CTAB, indicating that the solvent EG plays a very important role in the formation of Bi_2S_3 nanorods. Once the Bi_2S_3 nuclei formed, EG can effectively cap and stabilize the surface of the Bi_2S_3 nuclei via hydroxyl groups of the solvent molecules, which was beneficial for the preparation of stable and uniform Bi_2S_3 nanorods. Due to the effects of the hydrogen bonding between hydroxyl groups, EG molecules could exist in long chains and act as a soft template, leading to the growth of Bi_2S_3 nuclei into nanorods, similar to the function of DEG [27]. That is why there are no significant changes in morphology after 3, 7, 13, and 20 min of microwave heating in EG, as well as no difference in the presence and absence of CTAB.

Our previous study indicated that the bismuth precursor was very important to the formation of Bi_2S_3 nanorods. It was also confirmed by the observations in this study. In the microwave synthesis, $Bi(NO_3)_3$ dissociates into Bi^{3+} and NO_3^- ions immediately under the ambient conditions of DMF. Then the nucleation occurs when Tu decomposes to S^{2-} ions at an outburst speed, leading to the quick formation of a large quantity of Bi_2S_3 nuclei which works against the fabrication of individual Bi_2S_3 nanorods. However, there are few free Bi^{3+} ions when bismuth citrate is dispersed in DMF, resulting in little opportunity of reacting with Tu directly. Hence, large quantities of Bi^{3+} ions are conductive to formation of Bi_2S_3 nanorods in microwave synthesis. Similarly, few free Bi^{3+} ions were generated from $BiCl_3$ due to the hydrolysis of $BiCl_3$ to BiOCl in the initial reaction stage in DMF, which has a pH value of 4. Based on the findings, the bismuth precursors can be divided into two groups. One is a bismuth compound with poor solubility in the solutions, such as Bi(cit) and BiOCl, which can only slowly release the Bi^{3+} ions during the microwave heating process. The other is a bismuth com-

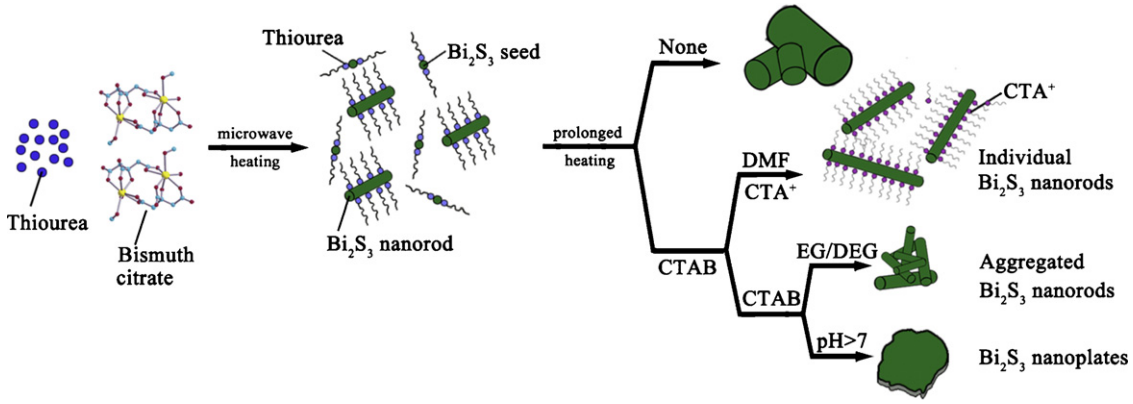

Scheme 1. Supposed formation process of the Bi_2S_3 nanorods.

pound, such as $Bi(NO_3)_3$, which can rapidly release the Bi^{3+} ions in the reaction system.

It was found that Bi_2S_3 nanorods were fabricated only by using Tu as sulfur precursor, indicating that slow release of S^{2-} would benefit the formation of Bi_2S_3 nanorods. It is well known that only Na_2S can directly give S^{2-} ions in the solvent, leading to the quick formation of Bi_2S_3 nuclei. Similar to Na_2S, ${S_2O_3}^{2-}$ ions come from $Na_2S_2O_3$ could react with H^+ ion in the reaction solution, which also induced the releasing of S^{2-} ions ($2H^+ + {S_2O_3}^{2-} \xrightarrow{\Delta} S^{2-} + 2H^+ + {SO_3}^{2-}$) [30]. The quick production of S^{2-} ions in these two precursors is not beneficial for the formation of Bi_2S_3 nanorods. When GSH was used as a precursor, the lone electron pair of the S atom of GSH strongly interacted with the Bi_2S_3 nuclei surface. The long hydrophilic carboxyl and amidogen tails formed a steric barrier and prevented the production of many excessive S^{2-} ions in the reaction system, resulting in a relatively slow reaction rate between S^{2-} ions and Bi(cit). However, no Bi_2S_3 nanorod was obtained in the presence of GSH. It was proposed that the steric hindrance effect of GSH prevented the fabrication of rod-like nanostructures. At the same time, the formation and in situ decomposition of Bi–GSH complex resulted in the fabrication of flower-like Bi_2S_3 nanostructures. In the literature, it was also reported that L-cysteine was used as a sulfur precursor and self-sacrificed templates to produce the interesting CuS nanostructures [74].

Small organic molecules which can slowly release S^{2-} by hydrolysis are especially useful in the controlled synthesis of Bi_2S_3 nanomaterials because of their special chemical properties and self-assembling functions [75]. It was reported that the S^{2-} ions generate slowly due to the cleavage of C=S bond of Tu [76]. During this reaction, the Tu gradually decomposes to release S^{2-} ions slowly as the temperature increases, preventing the production of too many free S^{2-} ions. At the same time, due to the excessive amount of Tu in the system, the lone electron pair of the S atom can strongly interact with and selectively adhere to the Bi_2S_3 nuclei surface. This can stabilize some special crystalline facets and these crystalline facets are electronegative, as indicated in the following equations:

$$(H_2N)_2C{=}S \xrightarrow{\Delta} S^{2-} + N{\equiv}CNH_2 + 2H^+$$

$$2Bi^{3+} + 3S^{2-} \rightarrow Bi_2S_3$$

Furthermore, almost no free Bi^{3+} ions are available in DMF owing to the unique coordination by citrate anions. These reasons resulted in the relatively slow reaction rate of formation Bi_2S_3 nuclei, leading to the aggregation of Tu on the existing Bi_2S_3 nuclei and resulting in the increase of their dimensions.

The results also indicated that Tu, which attached on Bi_2S_3 seeds, can act as another kind of capping agent to control the growth rate and morphology of Bi_2S_3 nanorods under microwave irradiation. We proposed that the larger quantity of Tu adsorbed on Bi_2S_3 seeds by electrostatic effect of the lone electron pair of the S atom is beneficial for the formation of "growing seeds" and the aspect ratio control. As a result, the growth of such an anisotropic structure requires a relatively high chemical potential environment, i.e., high monomer concentration in the solution. This may also explain why the aspect ratio increased with the increase of reaction time under microwave heating (**S1**–**S4**). Tu can thus also act as a shape controller in the formation of Bi_2S_3 nanorods. Therefore, it was seen that Tu plays an important role in the formation of Bi_2S_3 nanorods and high concentrations of Tu favor the growth of Bi_2S_3 nanorods.

4.2. Formation mechanism of the Bi_2S_3 nanorods

Based on the observations of the products under different experimental conditions, a proposed formation mechanism of the Bi_2S_3 nanorods under different condition was summarized in Scheme 1. As illustrated in this scheme, Bi_2S_3 nuclei were formed quickly under microwave heating, and with the help of Tu at the first stage, were subsequently preferential in the growth of Bi_2S_3 nanorods. At this stage, excessive Tu stabilized the Bi_2S_3 nuclei and promoted the growth of Bi_2S_3 nanorods though the adherence to the Bi_2S_3 nuclei surface. In the presence of CTAB, CTA^+ ions were generated in DMF, which were capped on the surface of Bi_2S_3 nanorods and led to the formation of long Bi_2S_3 nanorods with good dispersity with the increase of reaction time. At the same time, DEG also acted as a soft template in the formation of Bi_2S_3 nanorods. The poor solubility of CTAB and the high pH value of formamide and ethylenediamine resulted in the aggregation of Bi_2S_3 nanomaterials. However, the poor solubility of CTAB in EG did not affect the formation of Bi_2S_3 nanorods. Instead of CTAB, EG also played the role of capping agent, leading to the fabrication of Bi_2S_3 nanorods.

5. Conclusions

In this study, microwave irradiation, where energy is delivered to the reactants through molecular interactions with electromagnetic field, was found to be a convenient, efficient, and environmentally friendly route for the formation of Bi_2S_3 nanorods, as well as a new method of quick synthesis of other bismuth nanomaterials. A possible growth mechanism of Bi_2S_3 nanorods was also proposed in this study. Large-scale, well-separated Bi_2S_3 nanorods were successfully prepared from bismuth citrate and Tu by a microwave heating method. Microwave irradiation was found to reduce the reaction time by at least 80% compared with refluxing

under identical reaction conditions. CTAB and β-CD were found to facilitate the formation of Bi_2S_3 nanorods. DMF, EG and DEG are friendly solvents in the synthesis of Bi_2S_3 nanorods. The amount of Tu has a strong influence on the formation of Bi_2S_3 nanorods. It was also found that the dimensions of Bi_2S_3 are highly dependent on the bismuth and sulfur species. During the synthesis, the reaction time, surfactant, and solvent played important roles on the morphologies and dispersities of Bi_2S_3 nanomaterials. This new approach is believed to offer a more attractive, convenient, quick method for large-scale synthesis of Bi_2S_3 nanorods, and provide some useful clues for designing 1D nanostructural materials.

Acknowledgements

This work was supported by National Natural Science Foundation of China (Grant 20801043), Program for New Century Excellent Talents in University (NCET-09-0136) and Wuhan Chenguang Scheme (Grant 200850731376) established under Wuhan Science and Technology Bureau. We thank Mr. Frankie Y.F. Chan for his kind help with TEM characterizations.

Appendix A. Supplementary data

Supplementary data associated with this article can be found, in the online version, at doi:10.1016/j.jallcom.2010.10.160.

References

[1] S.-C. Liufu, H.-Y. Chen, Q. Yao, C.-F. Wang, Appl. Phys. Lett. 90 (2007), 112106.1–112106.3.
[2] G. Konstantatos, L. Levina, J. Tang, E.H. Sargent, Nano Lett. 8 (2008) 4002–4006.
[3] S.K. Batabyal, C. Basu, A.R. Das, G.S. Sanyal, J. Nanosci. Nanotechnol. 7 (2007) 565–569.
[4] X. Yu, C. Cao, Cryst. Growth Des. 8 (2008) 3951–3955.
[5] J.D. Desai, C.D. Lokhande, Mater. Chem. Phys. 41 (1995) 98–103.
[6] G. Hodes, J. Manassen, D. Cahen, Nature 261 (1976) 403–404.
[7] B. Miller, A. Heller, Nature 262 (1976) 680–681.
[8] O. Rabin, J. Manuel Perez, J. Grimm, G. Wojtkiewicz, R. Weissleder, Nat. Mater. 5 (2006) 118–122.
[9] C. Ye, G. Meng, Z. Jiang, Y. Wang, G. Wang, L. Zhang, J. Am. Chem. Soc. 124 (2002) 15180–15181.
[10] J.R. Ota, S.K. Srivastava, Nanotechnology 16 (2005) 2415–2419.
[11] Y.W. Koh, C.S. Lai, A.Y. Du, E.R.T. Tiekink, K.P. Loh, Chem. Mater. 15 (2003) 4544–4554.
[12] H. Bao, C.M. Li, X. Cui, Y. Gan, Q. Song, J. Guo, Small 4 (2008) 1125–1129.
[13] J.H. Kim, H. Park, C.-H. Hsu, J. Xu, J. Phys. Chem. C 114 (2010) 9634–9639.
[14] Z. Liu, S. Peng, Q. Xie, Z. Hu, Y. Yang, S. Zhang, Y. Qian, Adv. Mater. 15 (2003) 936–940.
[15] Z. Liu, J. Liang, S. Li, S. Peng, Y. Qian, Chem. Eur. J. 10 (2004) 634–640.
[16] A. Phuruangrat, T. Thongtem, S. Thongtem, Mater. Lett. 63 (2009) 1496–1498.
[17] Y. Zhao, X. Zhu, Y. Huang, S. Wang, J. Yang, Y. Xie, J. Phys. Chem. C 111 (2007) 12145–12148.
[18] Q. Lu, F. Gao, S. Komarneni, J. Am. Chem. Soc. 126 (2004) 54–55.
[19] F. Gao, Q. Lu, X. Meng, S. Komarneni, J. Mater. Sci. 43 (2008) 2377–2386.
[20] J. Wu, F. Qin, F.Y.F. Chan, G. Cheng, H. Li, Z. Lu, R. Chen, Mater. Lett. 64 (2010) 287–290.
[21] C. An, S. Wang, Y. Liu, Mater. Lett. 61 (2007) 2284–2287.
[22] Y. Jiang, Y.-J. Zhu, J. Phys. Chem. B 109 (2005) 4361–4364.
[23] J. Lu, Q. Han, X. Yang, L. Lu, X. Wang, Mater. Lett. 61 (2007) 3425–3428.
[24] F. Wei, J. Zhang, L. Wang, Z.-K. Zhang, Cryst. Growth Des. 6 (2006) 1942–1944.
[25] W. Lou, M. Chen, X. Wang, W. Liu, Chem. Mater. 19 (2007) 872–878.
[26] Y. Yu, C.H. Jin, R.H. Wang, Q. Chen, L.M. Peng, J. Phys. Chem. B 109 (2005) 18772–18776.
[27] H. Zhang, L. Wang, Mater. Lett. 61 (2007) 1667–1670.
[28] J. Wang, Y. Li, Mater. Chem. Phys. 87 (2004) 420–423.
[29] M. Salavati-Niasari, D. Ghanbari, F. Davar, J. Alloys Compd. 488 (2009) 442–447.
[30] H. Wang, J.-J. Zhu, J.-M. Zhu, H.-Y. Chen, J. Phys. Chem. B 106 (2002) 3848–3854.
[31] J.M. Zhu, K. Yang, J.J. Zhu, G.B. Ma, X.H. Zhu, S.H. Zhou, Z.G. Liu, Opt. Mater. 23 (2003) 89–92.
[32] X. Yu, C. Cao, H. Zhu, Solid State Commun. 134 (2005) 239–243.
[33] R. Chen, M.H. So, C.-M. Che, H. Sun, J. Mater. Chem. 15 (2005) 4540–4545.
[34] J. Zhu, O. Palchik, S. Chen, A. Gedanken, J. Phys. Chem. B 104 (2000) 7344–7347.
[35] X. Hu, J.C. Yu, Chem. Mater. 20 (2008) 6743–6749.
[36] J.A. Gerbec, D. Magana, A. Washington, G.F. Strouse, J. Am. Chem. Soc. 127 (2005) 15791–15800.
[37] X. Hu, J.C. Yu, J. Gong, J. Phys. Chem. C 111 (2007) 11180–11185.
[38] S. Komarneni, R. Roy, Q.H. Li, Mater. Res. Bull. 27 (1992) 1393–1405.
[39] S. Komarneni, R. Pidugu, Q.H. Li, R. Roy, J. Mater. Res. 10 (1995) 1687–1692.
[40] S. Komarneni, M.Z. Hussein, C. Liu, E. Breval, P.B. Malla, Eur. J. Solid State Inorg. Chem. 32 (1995) 837–849.
[41] S. Beg, A. Al-Alas, N.A.S. Al-Areqi, J. Alloys Compd. 493 (2010) 299–304.
[42] T. Thongtem, C. Pilapong, J. Kavinchan, A. Phuruangrat, S. Thongtem, J. Alloys Compd. 500 (2010) 195–199.
[43] J. Wu, H. Yang, H. Li, Z. Lu, X. Yu, R. Chen, J. Alloys Compd. 498 (2010) L8–L11.
[44] Q. Yao, Y. Zhu, L. Chen, Z. Sun, X. Chen, J. Alloys Compd. 481 (2009) 91–95.
[45] F.Y. Jiang, C.M. Wang, Y. Fu, R.C. Liu, J. Alloys Compd. 503 (2010) L31–L33.
[46] G. Wei, W. Qin, D. Zhang, G. Wang, R. Kim, K. Zheng, L. Wang, J. Alloys Compd. 481 (2009) 417–421.
[47] C.-H. Lu, B. Bhattacharjee, S.-Y. Chen, J. Alloys Compd. 475 (2009) 116–121.
[48] J. Bi, L. Wu, Z. Li, Z. Ding, X. Wang, X. Fu, J. Alloys Compd. 480 (2009) 684–688.
[49] S. Komarneni, Curr. Sci. India 85 (2003) 1730–1734.
[50] S.A. Galema, Chem. Soc. Rev. 26 (1997) 233–238.
[51] M. Tsuji, M. Hashimoto, Y. Nishizawa, M. Kubokawa, T. Tsuji, Chem. Eur. J. 11 (2005) 440–452.
[52] Y. Jiang, Y.-J. Zhu, Z.-L. Xu, Mater. Lett. 60 (2006) 2294–2298.
[53] X.-H. Liao, H. Wang, J.-J. Zhu, H.-Y. Chen, Mater. Res. Bull. 36 (2001) 2339–2346.
[54] T. Thongtema, A. Phuruangratb, S. Wannapopb, S. Thongtem, Mater. Lett. 64 (2010) 122–124.
[55] L. Cademartiri, R. Malakooti, G. Paul, A. O'Brien, Migliori S. Petrov, Nazir P. Kherani, G.A. Ozin, Angew. Chem. Int. Ed. 47 (2008) 3814–3817.
[56] Q. Han, J. Chen, X. Yang, L. Lu, X. Wang, J. Phys. Chem. C 111 (2007) 14072–14077.
[57] Z. Quan, J. Yang, P. Yang, Z. Wang, C. Li, J. Lin, Cryst. Growth Des. 8 (2008) 200–207.
[58] J. Jiang, S.-H. Yu, W.-T. Yao, H. Ge, G.-Z. Zhang, Chem. Mater. 17 (2005) 6094–6100.
[59] J. Black, E.M. Conwell, L. Seigle, C.W. Spencer, J. Phys. Chem. Solids 2 (1957) 240–251.
[60] D. Tseng, E. Ruckenstein, Mater. Lett. 8 (1989) 69–71.
[61] H. Mizoguchi, H. Hosono, N. Ueda, H. Kawazoe, J. Appl. Phys. 78 (1995) 1376–1378.
[62] S.-H. Yu, L. Shu, J. Yang, Z.-H. Han, Y.-T. Qian, Y.-H. Zhang, J. Mater. Res. 14 (1999) 4157.
[63] Y. Huang, W. Wang, H. Liang, H. Xu, Cryst. Growth Des. 9 (2009) 858–862.
[64] Y. Xie, X. Zheng, X. Jiang, J. Lu, L. Zhu, Inorg. Chem. 41 (2002) 387–392.
[65] Z. Zhang, B. Zhao, L. Hu, J. Solid State Chem. 121 (1996) 105–110.
[66] H. Xue, Z. Li, H. Dong, L. Wu, X. Wang, X. Fu, Cryst. Growth Des. 8 (2008) 4469–4475.
[67] Y. Sun, Y. Xia, Science 298 (2002) 2176–2179.
[68] I. Washio, Y. Xiong, Y. Yin, Y. Xia, Adv. Mater. 18 (2006) 1745–1749.
[69] C.E. Hoppe, M. Lazzari, I. Pardinas-Blanco, M.A. Lopez-Quintela, Langmuir 22 (2006) 7027–7034.
[70] Y. Horiguchi, K. Honda, Y. Kato, N. Nakashima, Y. Niidome, Langmuir 24 (2008) 12026–12031.
[71] S.K. Batabyal, C. Basu, G.S. Sanyal, A.R. Das, Mater. Lett. 58 (2003) 169–171.
[72] J. Madarász, P. Bombicz, M. Okuya, S. Kaneko, G. Pokol, J. Anal. Appl. Pyrol. 72 (2004) 209–214.
[73] J. Madarász, P. Bombicz, M. Okuya, S. Kaneko, G. Pokol, Solid State Ionics 172 (2004) 577–581.
[74] B. Li, Y. Xie, Y. Xue, J. Phys. Chem. C 111 (2007) 12181–12187.
[75] P. Bombicz, I. Mutikainen, M. Krunks, T. Leskelä, J. Madarász, L. Niinistö, Inorg. Chim. Acta 357 (2004) 513–525.
[76] L. Dong, Y. Chu, Y. Liu, L. Li, J. Colloid Interface Sci. 317 (2008) 485–492.